Applied Nanoscience (2022) 12:129–138
https://doi.org/10.1007/s13204-021-02249-w

ORIGINAL ARTICLE

All-green wound dressing prototype based on Nile tilapia skin impregnated with silver nanoparticles reduced by essential oil

Milena Lima Guimarães[1] · Fernando Antonio Gomes da Silva Jr.[1] · Anderson Miranda de Souza[1] · Mateus Matiuzzi da Costa[1] · Helinando Pequeno de Oliveira[1]

Received: 2 April 2021 / Accepted: 13 November 2021 / Published online: 2 December 2021

Abstract
The development of eco-friendly prototypes for wound dressing systems represents an important source of investigation about alternatives for the treatment of severe infections. The production of antibacterial agents free of antibiotics, based on natural products and biological supports is a hot topic for science applied in circular economy concepts. Herein, the green synthesis of silver nanoparticles was assisted by essential oil and the following impregnation of products in tilapia skin has been conducted as a strategy to produce all-green wound dressing systems to be applied as biofilm protective layers and active antibacterial agents. The use of these wound dressing systems against *Staphylococcus aureus* was evaluated in terms of biofilm adhesion, inhibition halo assays, and time-kill assays as a function of the nature of reducing agent applied in the production of silver nanoparticles.

Keywords Silver nanoparticles · Essential oil · Tilapia fish skin · Wound dressing · Antibacterial · Biofilm

Introduction

The increasing interest for investigation about smart dressings paves way for the development of therapeutic solutions to treat chronic infections (Ferrag et al. 2021; Hussain et al. 2017; Mao et al. 2021; Ochoa et al. 2020; van Wamel 2017) The skin is considered the major surface organ of the human body and is responsible by protecting the inner tissues from physical, chemical, and biological dangers (Chambers and Vukmanovic-Stejic 2020). In some cases, in which the skin integrity is lost, the healing of chronic wounds is a complex and slow process, that involves multiple cellular mediators and a set of well-organized phases in the coagulation and anti-inflammatory processes, and in the reconstruction of new tissues (Asati and Chaudhary 2017; Ciecholewska-Juśko et al. 2021; Hussain et al. 2017; Roy et al. 2021). This is a serious health problem and is a life-threatening disease with rough prevalence and mortality (Sharifi et al. 2021).

Examples of innovation in wound dressings are the incorporation of silver nanoparticles into hydrogel matrices with enhanced antimicrobial and mechanical properties (Ferrag et al. 2021), electroanalytical flexible dressing based on conductive nanocomposites for monitoring bacterial infections (Roy et al. 2021), natural polymer-based films with antioxidant properties (Bergonzi et al. 2020), up to the use of cross-linked superabsorbent bacterial cellulose-based biomaterials for the treatment of chronic wounds (Ciecholewska-Juśko et al. 2021).

Nile tilapia skin is an innovative natural product with the potential for application in cell regeneration and proliferation (Hu et al. 2017; Miranda and Brandt 2019; Ouyang et al. 2018; Song et al. 2021). With a similar morphological structure to human skin, non-infectious microbiota, and a large amount of type I collagen, tilapia skin has been applied to the treatment of burns (Lima et al. 2020; Ouyang et al. 2018; Song et al. 2019) control of bleeding in consequence of blood clotting ability/ hemostatic efficiency (Sun et al. 2020), and wound healing (Wang et al. 2021).

In terms of wound healing applications, it is important to evaluate the antibacterial activity of different materials. Chronic wounds are susceptible to infections, mainly caused by *Staphylococcus aureus*, a Gram-positive bacteria that impairs the healing process (Abele-Horn et al. 2000; Fazli

✉ Helinando Pequeno de Oliveira
helinando.oliveira@univasf.edu.br

[1] Institute of Materials Science, Universidade Federal do Vale do São Francisco, Avenida Antônio Carlos Magalhães, 510 Santo Antônio, Juazeiro, BA CEP 48902-300, Brazil

et al. 2009; James et al. 2008; Roy et al. 2021). Biofilms are associated with chronic nonhealing wound infections and have been considered a big challenge for the development of conventional therapy, stressing the necessity of new alternative antimicrobial strategies (Evelhoch 2020). An efficient way to increase the antibacterial activity of tilapia skin and its functionality as a material for biomedical application is based on its association with silver nanoparticles. Silver nanoparticles (AgNPs) play an important role as alternative antibacterial agents against *S. aureus*, and *Streptococcus pyogenes* (Gram-positive bacteria), as well as efficiency against Gram-negative bacteria, such as *Escherichia coli*, (Schierle et al. 2009) *Pseudomonas aeruginosa,* and *Klebsiella pneumonia*e (Maghimaa and Ali 2020; Nishanthi et al. 2018).

The synthesis of silver nanoparticles is divided into conventional methods (chemical, phytochemical and physical) and unconventional (biological) methods. Ion reduction by conventional methods is based on microemulsions, thermal degradation, electrochemical synthesis, evaporation–condensation, etc. (Tulinski and Jurczyk 2017) The biological method (or green synthesis) is based on the use of plant extracts (Guimarães et al. 2020), essential oils (Maciel et al. 2019), bacteria, fungi, algae (Abdelghany et al. 2018) and organic biomolecules (Salaheldin et al. 2017) for the reduction of silver ions.

The green synthesis of metal nanoparticles has been progressively reported in the literature, representing one of the most important eco-friendly alternatives for the production of AgNPs. The overall process of metal nanoparticle synthesis can be mediated by essential oils, that offers a diversity of chemical components (phenolic acids, flavonoids, terpenoids, and anthocyanins) applied in the steps of nucleation, growth, and stabilization of nanoparticles, with the possibility of incorporation of synergistic processes in antibacterial activity of synthesized AgNPs (Mukundan et al. 2005; Vilas et al. 2016, 2014). The association of eco-friendly silver nanoparticles and natural materials as supports for wound dressing prototypes represents a promising strategy to reach desirable antibacterial activity against severe infections.

Herein, an environmentally friendly method is proposed for the production of silver nanoparticles followed by a step of impregnation of these nanostructures in Nile tilapia skin, which has been applied as a smart wound dressing system against *S. aureus*. For this, the optimization in the essential oil (type and concentration) was evaluated in terms of the response of synthesized samples (morphology, structure, and optical response), while the association of these nanoparticles with Nile tilapia was evaluated in terms of effective activity as an antibacterial and antibiofilm agent. The general scheme for procedures explored in this work is summarized in Fig. 1, in which is possible to identify the green synthesis of silver nanoparticles, the impregnation in tilapia skin for the following step of the use of resulting material as support in antibacterial assays.

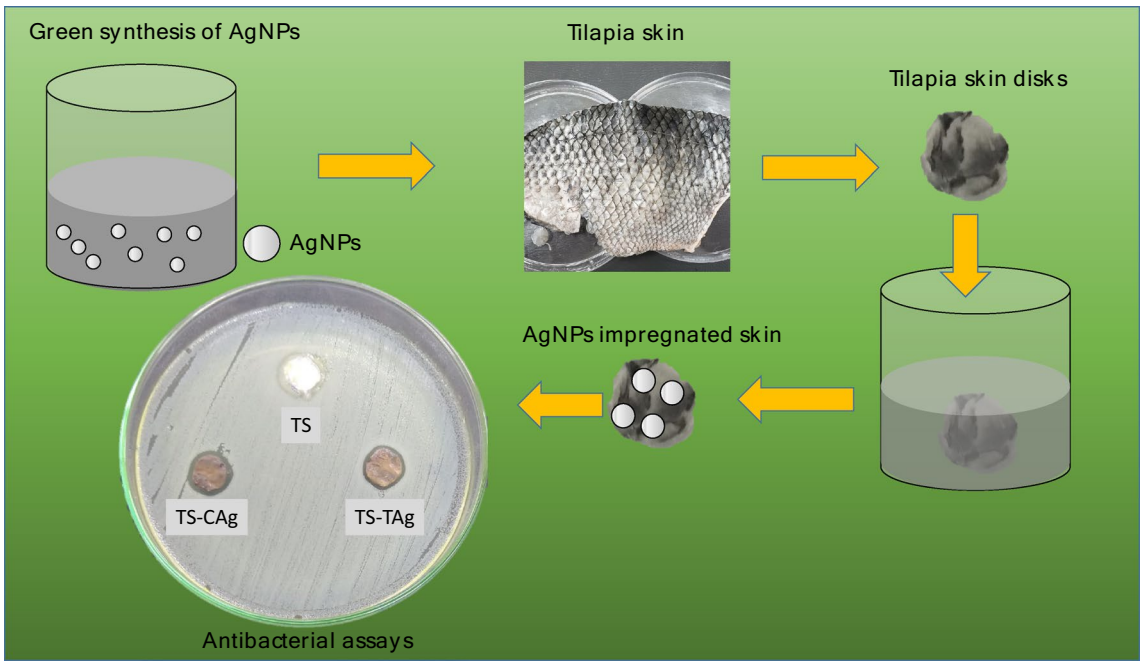

Fig. 1 General scheme for the synthesis and impregnation of silver nanoparticles into tilapia fish skin and the following step of use for in vitro assays against bacteria

Materials and methods

Materials

Silver nitrate (Sigma Aldrich), sodium hydroxide, and acetone (Dinâmica, Brasil) all PA degrees were used as received. Ultrapure water was produced from the Millipore system (Millipore, USA) with a resistivity of 18 MΩcm. The essential oil of *Cymbopogon nardus*, *Melaleuca alternifolia, Eucalyptus globulus, Eugenia caryophyllus,* and *Cinnamomum zeylanicum* were acquired from Akã Óleos Essenciais (Bahia, Brazil), with a high degree of purity.

Green synthesis of silver nanoparticles

Silver nanoparticles were biosynthesized according to the method described by Maciel et al. (2019) with some modifications. An initial group of five essential oils (*Cymbopogon nardus*, *Melaleuca alternifolia, Eucalyptus globulus, Eugenia caryophyllus,* and *Cinnamomum zeylanicum*) was explored as active agents for the reduction of the silver nanoparticles. An effective activity for the silver reduction was observed for tea tree oil (*Melaleuca alternifolia*) and citronella oil (*Cymbopogon nardus*). As a general standard method, aliquots of both essential oils (100 µL) were diluted in 17 mL of acetone at pH 8 which was adjusted from the incorporation of NaOH aqueous solution (0.1 M). Following this step, an aqueous solution of silver nitrate (1 mM) was prepared from which an aliquot of 30 mL was removed and kept under intense stirring and heating (95 °C).

After this step, solutions of essential oils (tea tree and citronella) were dropwise into silver nitrate aqueous solution until reaching a total volume of 32 mL (2 mL of essential oil solution). The kinetics of the formation of silver nanoparticles was monitored at a fixed interval of time (15, 30, 45, and 60 min) from the measurement of the characteristic peak of absorbance of silver nanoparticles in the UV–Vis spectrum. To avoid the effect of degradation induced by light, all of the procedures were conducted in dark conditions. The resulting samples of silver nanoparticles were identified as TAg (tea tree oil-based silver nanoparticles) and CAg (citronella oil-based silver nanoparticles).

Preparation of tilapia fish skin (TS)

Nile tilapia fish skins were donated by Omega Pescados do Vale (Brazil) and treated as follows: fish scales and the excess of residual fish meat were removed with a stiletto. In the following step, disks of TS with a 2 cm-diameter were separated and washed with ultrapure water in abundance and immersed in a phosphate saline solution (PBS) a 37° C. These steps are based on the procedure reported by (Howaili et al. 2020) (with some modifications).

Impregnation of silver nanoparticles on Nile tilapia fish skin

The impregnated Nile tilapia skin with different silver nanoparticles (TAg and CAg)—defined as TS-TAg and TS-CAg (respectively), were prepared as follows: circular disks of TS were immersed into as-prepared silver nanoparticle solution at a fixed interval of time, in a process that induces the adsorption of nanoparticles into the tilapia skin. The resulting material was dried at ambient temperature to eliminate residual water.

Characterization methods

The absorption spectra of silver nanoparticles in water were measured by a UV–Vis HachDR500 spectrophotometer in the range of 300–800 nm (step of 1 nm). The nanoparticles' size, zeta potential, and dispersity index were determined in a zetasizer Nano-ZS90 Malvern. The structure of synthesized material was scrutinized by FTIR assays, using the KBr method in a Fourier Transform Infrared spectrometer IR Prestige-21 Shimadzu.

Antibacterial assays

Bacterial cultures of *S. aureus* (ATCC 25923-reference for strong biofilm formation) were kept at 40 ^{0}C in stock solutions from which aliquots were removed to prepare saline aqueous solutions (0.5 in McFarland scale of turbidity). Aliquots of this solution were removed to be inoculated on Muller–Hinton agar plates (10^4–10^8 CFU). Qualitative evaluation of the activity of silver nanoparticles impregnated in tilapia skin was performed from inhibition halo experiments, in which circular disks of tilapia skin fish (negative control), TS-TAg, and TS-CAg samples were disposed on a Petri dish with Plate Count Agar (PCA) in the presence of *S. aureus* for 24 h at 37 ^{0}C. Biofilm formation quantification was evaluated according to (Da Silva et al. 2016) in which tryptic soy broth (TSB) solution + glucose aqueous solution (0.25 wt%) received *S. aureus* (10^7 CFU/mL) and the disks of tilapia skin (negative control), TS-TAg and TS-CAg which were inoculated for 24 h at 37° C. After this process, the resulting skin and reactor were immersed in a solution of crystal violet (0.25 wt% in water) to target the biofilm surface with the dye. Then, the skin and the reactor were washed with water to remove non-adhered species. The biofilm formation

was evaluated from absorbed (and colored) species that were removed from surfaces with a solution of 80:20 of alcohol: acetone. The intensity of absorbance at 570 nm was explored as a parameter for the identification of the number of adhered species.

The kinetics of bacterial growth was determined from the dispersion of viable cells into the saline solution and the time of interaction with an antibacterial agent (TAg and CAg). After a fixed interval of time (1 h, 2 h, 3 h, 4 h, and 5 h), an aliquot of 100 mL of the resulting dilution was inoculated in PCA for 24 h at 37 ^{0}C. After that, the remaining CFU was counted by direct inspection of the remaining viable cells, as reported in Ref. (da Silva et al. 2019).

Results and discussion

Surface plasmon resonance band formation

The surface plasmon resonance (SPR) phenomena observed in metal nanoparticles make use of the confinement of electromagnetic field near the metal nanoparticles surface as an important tool for the in-situ monitoring of the synthesis of silver nanoparticles by UV–visible spectroscopy. The intensity and the typical band shift of the characteristic peak around 410 nm depend on several factors, such as the size of nanoparticles, shape, and aggregation level (Granbohm et al. 2018; Guimarães et al. 2020).

Based on these relevant properties, the kinetics of silver nanoparticle formation was evaluated at a fixed interval of 15 min from the measurement of the UV–Vis spectrum of the resulting solution. As shown in Fig. 2a, b, the intensity of the SPR band (observed at 420 nm for both samples) increases with the time of reaction, indicating the progressive nucleation and silver nanoparticles formation with the progressive reaction that is dependent on the action of a reducing agent component (Guimarães et al. 2020). The absorbance for TAg-based samples presents a general behavior indicating a lower amount of silver nanoparticles at the beginning of the reaction (see Fig. 2a), while for CAg-based samples, it is observed a stronger reaction for nanoparticles reduction (the initial absorbance level for CAg-based samples is in order of 4 × higher than TAg-based samples)—see Fig. 2b. The corresponding variation level in the absorbance of CAg is limited in the range of 2.14–2.76, while the variation for TAg-based samples is observed in the range of 0.48–1.43. The variation in the absorbance peak (at 420 nm) is plotted as a function of the time of reaction in Fig. 2c. As shown, despite a higher slope for TAg-based reaction, the more effective synthesis (in terms of density of synthesized nanoparticles) is observed for the CAg-based system in consequence of initial faster kinetics of nanoparticles nucleation and growth.

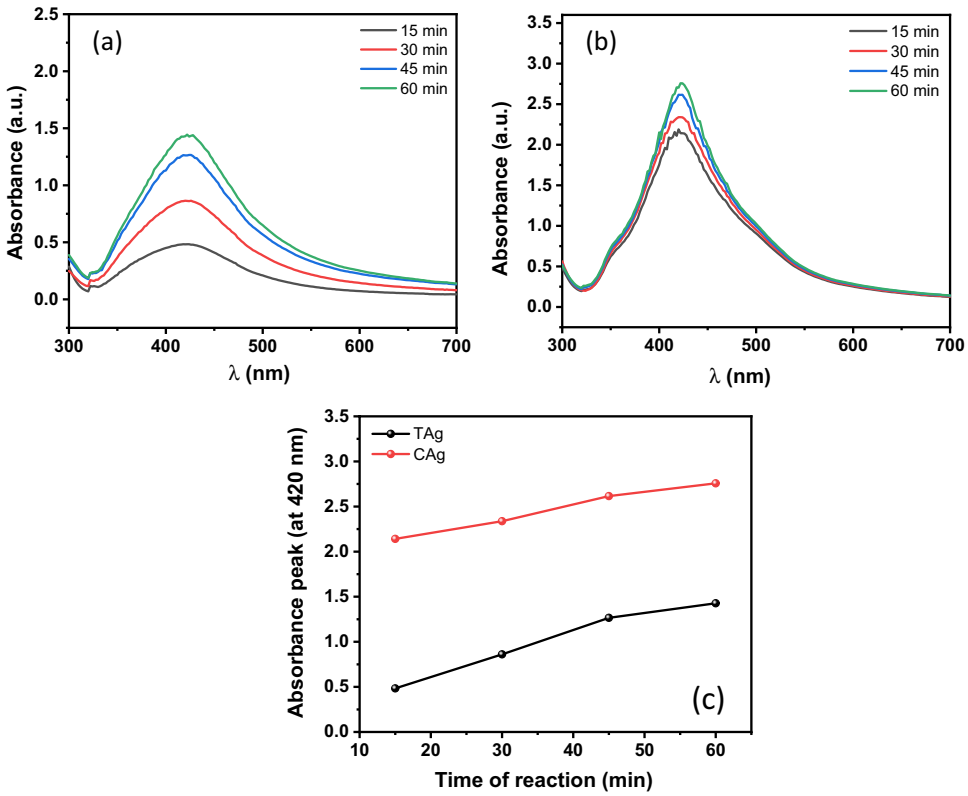

Fig. 2 Absorbance of silver nanoparticles solution in the UV–Vis region as a function of time of reaction (black—15 min, red—30 min, blue—45 min, and green—60 min) for TAg-based nanoparticles (**a**), CAg-based nanoparticles (**b**) and comparison of characteristic SPR band for TAg- and CAg-based nanoparticles as a function of time of reaction (**c**)

Morphology and size distribution of synthesized nanoparticles

The size of nanoparticles, measured from dynamic light scattering (DLS), is summarized in Fig. 3. As can be seen, a unique distribution of the size of particles is observed for TAg-based silver nanoparticles that are centered around 39.41 nm with a zeta potential of -35.6 mV, while a two population of particles with specific size distribution is observed for CAg-based silver nanoparticles, that are centered at 1.81 nm and 45.64 nm with a zeta potential of − 27.8 mV. As a consequence of this distribution, the polydispersity index (PDI value—which is a dimensionless measurement of the amplitude of the particle size distribution) is higher for CAg-based samples (0.554) than observed for TAg-based samples (0.287). An important aspect to be considered from these results concerns the available surface area for the synthesized nanoparticles, that present size in the order of nanometers, and favor the attachment of these structures on bacterial cell wall for the following step in which the number of viable cells tends to be strongly reduced (diffusion of ions into cells).

The process of impregnation of silver nanoparticles into TS samples results in a progressive change in color of the tilapia skin, that turns from grayscale to a brown aspect, as observed in Fig. 4a in which are compared the aspects of pure tilapia skin (TS) with the impregnated skin with TAg-based nanoparticles (TS-TAg) and modified skin with CAg-based nanoparticles (TS-CAg). The identification of the impregnated silver nanoparticles into tilapia skin was evaluated from EDS measurement. For comparison, it is shown in Fig. 4b, d, f the SEM images for tilapia skin, TS-TAg samples, and TS-CAg samples, respectively. The corresponding EDS map is shown in Fig. 4c, e, g, respectively.

As shown, the typical wrinkled surface of the tilapia skin (Fig. 4b) is preserved under impregnation with silver nanoparticles (Fig. 4d, f), that are identified from small metallic aggregates (regions in white) scrutinized in the EDS spectrum (Fig. 4e, g), confirming the impregnation of tilapia skin with silver nanoparticles.

Characterization of wound dressing systems (impregnated silver nanoparticles into tilapia skin)

The amount of adsorbed silver nanoparticles on tilapia skin was estimated from the direct measurement of SPR peak intensity of solution in the reactor before and after the process of nanoparticle adsorption on the skin. As shown in Fig. 5a, a variation in order 67.59% is observed for TAg-based samples, while 61.42% of the variation is observed for CAg-based samples. Despite higher performance in relative adsorption of silver nanoparticles for TAg-based nanoparticles, due to the higher amount of synthesized CAg-based nanoparticles (a higher value for SPR band), it is expected a higher density of CAg-based nanoparticles impregnated into tilapia skin samples.

The identification of additional components than silver that is impregnated in the tilapia skin (subproducts from bioreduction provided by essential oils) was measured by FTIR assays. For this, the spectrum of tilapia skin, TS-TAg, and TS-CAg were analyzed as follows. Figure 5b shows the FTIR spectrum of TS (curve in black), TS-TAg (curve in red), and TS-CAg (curve in blue). Bands at 2924 cm^{-1} and 2850 cm^{-1} correspond to the stretching vibration of =C–H group and arise from primary and secondary amines (Alfuraydi et al. 2019; Veisi et al. 2019), while bands at 1240 and 1550 cm^{-1} are assigned to the N–H vibration modes associated with C–N and C–H vibration from amide II and III from the collagen of Nile tilapia skin (Song et al. 2021). In addition, characteristic bands at 1382 cm^{-1} observed for TS-TAg and TS-CAg (samples impregnated with silver nanoparticles) are assigned to the carbonyl group and carboxylic acid which have a high affinity to Ag ions, acting as reducing and stabilizing agents for produced silver nanoparticles (Vilas et al. 2016, 2014). The band at 1175 cm^{-1} is associated with the stretching vibration of C–OH, which has been correlated with changes in the characteristic vibrations of

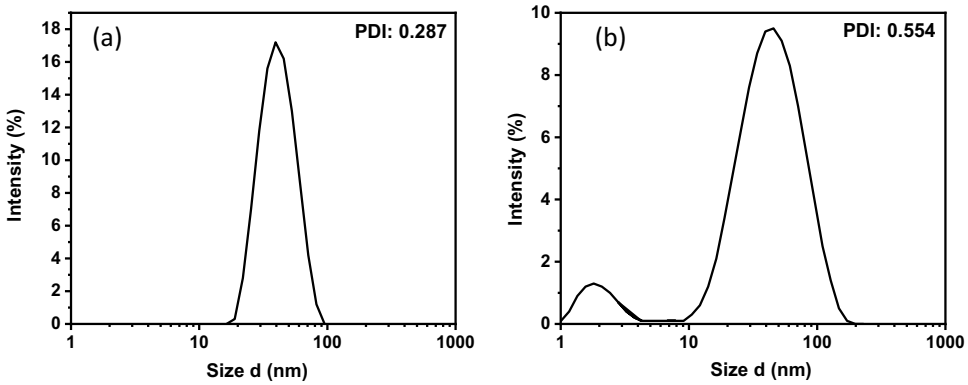

Fig. 3 DLS measurement showing the distribution of size of nanoparticles and PDI value for **a** TAg-based silver nanoparticles and **b** CAg-based silver nanoparticles

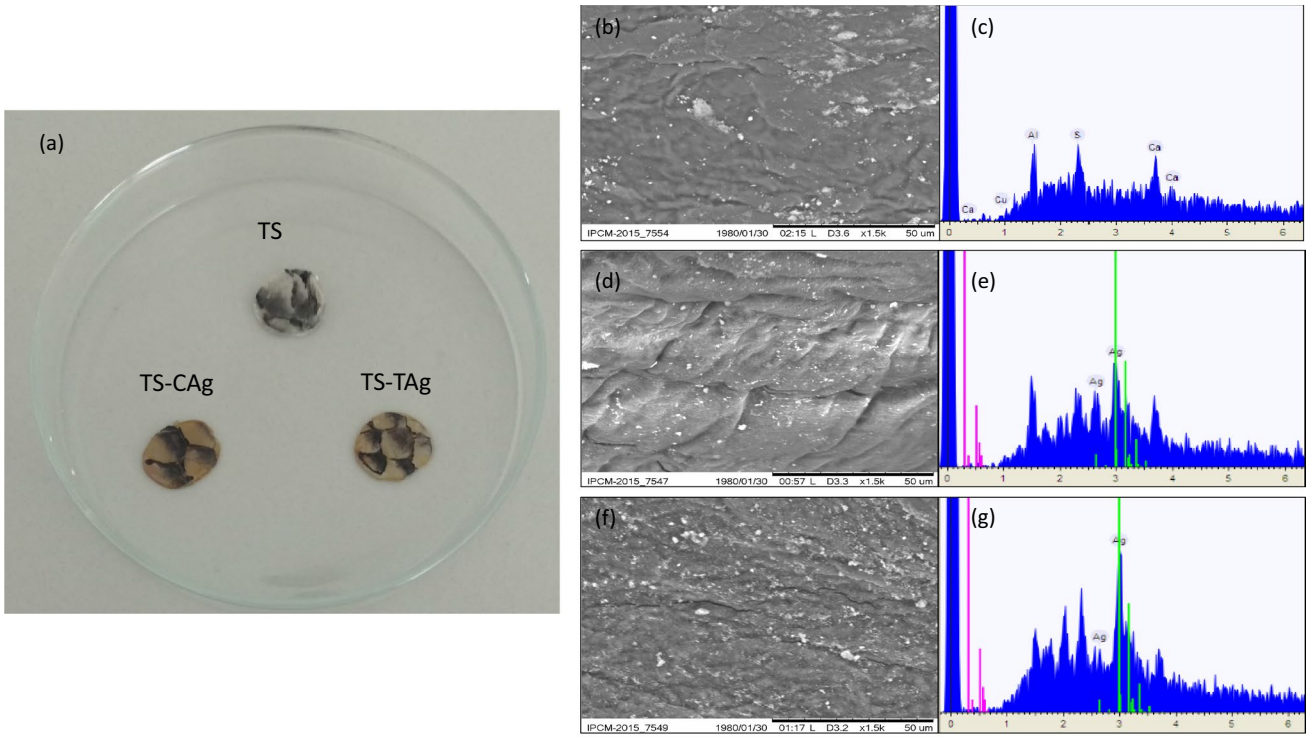

Fig. 4 **a** Photos of pure tilapia skin (TS), impregnated with CAg-based silver nanoparticles (TS-CAg) and with TAg-based silver nanoparticles (TS-TAg); **b** SEM image of pure tilapia skin and **c** corresponding EDS spectrum; **d** SEM image of TAg-based modified tilapia skin and **e** corresponding EDS spectrum; **f** SEM image of CAg-based modified tilapia skin and **g** corresponding EDS spectrum

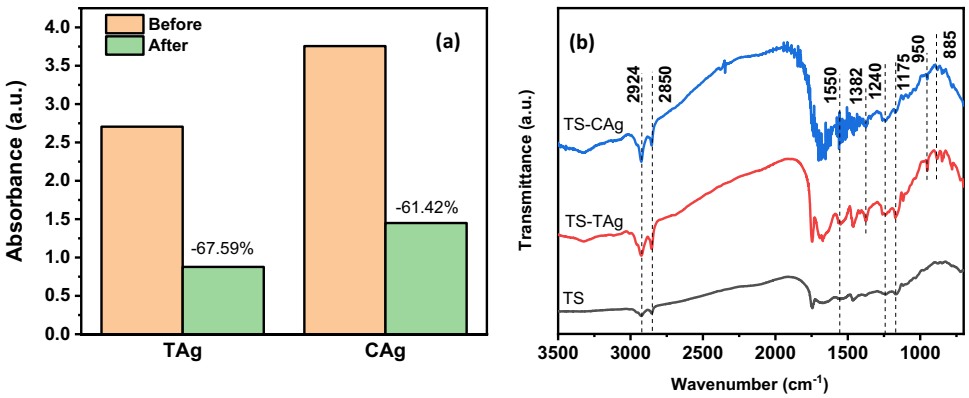

Fig. 5 **a** Comparison of the absorbance of silver nanoparticles dispersed in the reactor before and after the impregnation of silver nanoparticles into tilapia fish skin, **b** FTIR spectrum of pure tilapia skin (TS-curve in black), tilapia skin impregnated with TAg-based nanoparticles (TS-TAg-curve in red) and tilapia skin impregnated with CAg-based nanoparticles (TS-CAg-curve in blue)

carboxyl, phenol, and proteins from essential oils (Gavade et al. 2015). Characteristic vibration of the group $CH_3(CO)$, vibrations in the group C–O–C, and CH_2 are observed at 1087 cm^{-1} (Dzimitrowicz et al. 2016). The band at 950 cm^{-1} is assigned to heterocyclic compounds (Sutthanont et al. 2019), while bands at 885 cm^{-1} are assigned to C–O vibrations, and the band at 846 cm^{-1} is associated with out-of-plane vibration of N–H from amides (Gavade et al. 2015; Vilas et al. 2014). These bands confirm the presence of alcohol, carboxylic acid, phenolic acid, and heterocyclic compounds, which are active components for the complexation, nucleation, and growth of silver nanoparticles (Ahmad et al. 2013; Maghimaa and Ali 2020).

Antibacterial assays

The qualitative evaluation about antibacterial activity of TS-Ag-based systems was performed by measurement of inhibition haloes, in which circular disks of TS-TAg and TS-CAg are disposed of in plates inoculated with *S. aureus*. As shown in Fig. 6, for both systems are observed a discrete inhibition halo (in comparison with negative control), characterizing

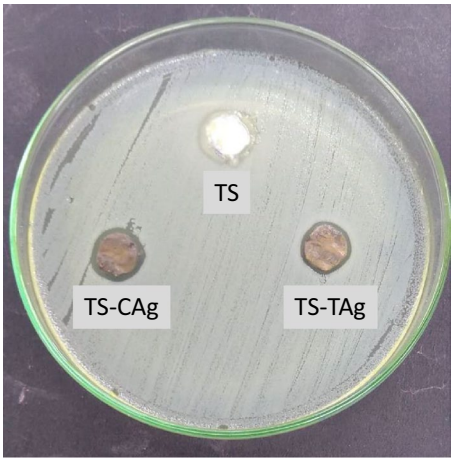

Fig. 6 Inhibition halo for control experiment (tilapia fish disk), TS-CAg, and TS-TAg disks

the diffusion of antibacterial active agents in direction of the bacterial viable cells. Moreover, negligible inhibition halo was observed for pure tilapia skin, characterizing the relevance of impregnated species. The antimicrobial activity of silver nanoparticles is associated with membrane binding, DNA damage, silver ions liberation, and oxidative stress (Tang and Zheng 2018).

In general, the most accepted hypothesis to explain the cytotoxicity of the silver nanoparticles is the Trojan horse mechanism (Jorge de Souza et al. 2019), a concentration-dependent mechanism based on the toxicity of released ions that migrates to the intracellular environment and damage lysosomes, with subsequent lesions in the cell membrane and genetic material, that justify the antibacterial activity for this material.

As a consequence, the treatment of skin wounds with silver nanoparticles alone or functionalized with diverse antimicrobial compounds has been demonstrated promising wound therapeutic effects (Li et al. 2019; Negut et al. 2018).

The quantification of the antibacterial activity of synthesized nanoparticles was evaluated from time-kill assays, in which an aqueous solution with 10^4 colonies of *S. aureus* received aliquots of synthesized nanoparticles at a determined time of reaction in a saline solution in the presence of silver nanoparticles. The resulting material was inoculated into plates at 37° C for 24 h for the posterior counting of viable cells. The treatment was fixed in the interval of time of 1 h, 2 h, 3 h, 4 h, and 5 h—for comparison, a negative control experiment was evaluated in the absence of antibacterial materials. As shown in Fig. 7a, a decrease in the order of 27% is observed in the number of viable cells for the control experiment. However, the reduction in the number of viable cells after treatment with both experimental systems (TAg and CAg) is in order of 73% after 5 h of contact with antibacterial material. The general behavior of the curves is the same, with an exponential decay that reaches saturation for a time in order of 5 h, characterizing a relevant reduction in the number of viable cells that confers an important application for synthesized nanoparticles.

On the other hand, *S. aureus* biofilm producers are involved in the pathogenesis of chronic wound infections (Mottola et al. 2016). These opportunistic pathogens live in skin biofilms and the use of conventional antimicrobial agents induces bacterial survival and the development of persistent infection (van Wamel 2017). Moreover, an important parameter to be evaluated is the antibiofilm activity of silver nanoparticles impregnated in tilapia fish skin. This activity was evaluated for negative control (tilapia fish), TS-TAg, and TS-CAg samples which were applied as a support for the removal of biofilm that could be attached to the reactor.

The measurement of variation in the relative biofilm adhesion for both surfaces (tilapia skin and reactor) was performed according to the comparative variation in the

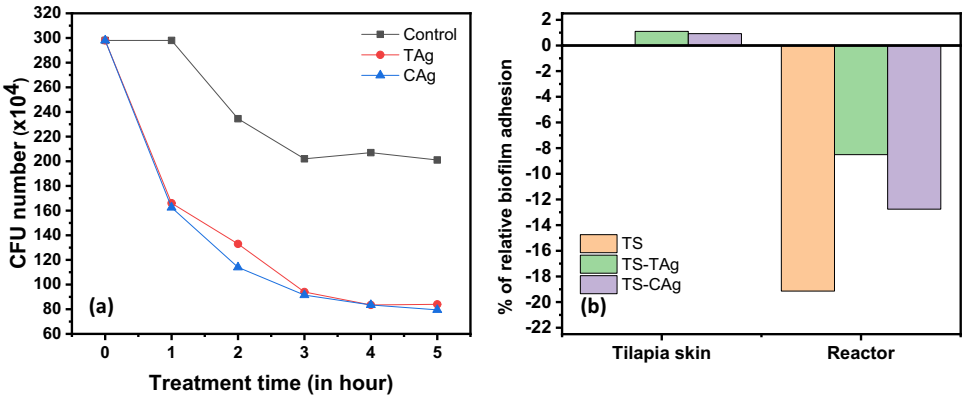

Fig. 7 **a** Time-kill assays performed to evaluate the characteristic time of action of synthesized nanoparticles (CAg and TAg) and **b** the variation in the biofilm adhesion degree on the sample (tilapia skin coated with nanoparticles) and on the reactor

absorbance of released dye molecules that target biofilm species. The percentage of variation in the biofilm adhesion (BA) is given by Eq. 1 (da Silva et al. 2019; dos Santos et al. 2018).

$$\%\mathrm{BA} = \left(\frac{A_{\mathrm{sample}} - A_{\mathrm{control}}}{A_{\mathrm{control}}}\right) * 100\% \quad (1)$$

where the negative control for tilapia skin is the absorbance of adhered targeted species on pristine tilapia skin, while the control for the reactor is measured in the absence of antibacterial agents. As shown in Fig. 7b, the relative variation in the biofilm adhesion on tilapia skin substrates is minimally affected by the incorporation of silver nanoparticles. A positive variation in the order of 1% in biofilm adhesion degree is attributed to the impregnation of silver nanoparticles on tilapia skin. On the other hand, a strong reduction in the biofilm formation on the reactor is observed as a result of interaction with pristine tilapia skin (control experiment) in order of 19%. The impregnation of tilapia skin with silver nanoparticles reduces this efficiency to values in order of 9% (TS-TAg) and 13% (TS-CAg). This process is a consequence of the filling of active sites for biofilm adsorption with silver nanoparticles that favor the antibacterial activity against planktonic form (Estevez et al. 2020; Le Ouay and Stellacci 2015). These results suggest that impregnated silver nanoparticles in tilapia skin associate its intrinsic antibacterial activity with antibiofilm properties, characterizing an important combination of mechanisms for this prototype of wound dressing system.

Conclusion

The impregnation of "green" silver nanoparticles into tilapia skin as prototypes of wound dressing systems introduces a promising procedure that associates the antibacterial activity of silver nanoparticles with the antibiofilm activity of chemically modified tilapia fish skin on reactor, in a system that can be considered as a candidate for the treatment of severe infections. The use of natural materials for the preparation of silver nanoparticles and the development of the tilapia skin-based wound dressing represents an important trend preconized by the science for a circular economy that is favored by the use of free-antibiotic and low-cost systems. The reduction in the viable cells of 73% in association with the reduction in the biofilm formation (in order of 19%) represents two important parameters that can be synergistically explored from this new platform for all-green wound dressing systems.

Acknowledgements This work was supported by CAPES, FACEPE, FINEP and CNPq.

Declarations

Conflict of interest The authors have declared no conflict of interest.

References

Abdelghany TM, Al-rajhi AMH, Al AMA (2018) Recent advances in green synthesis of silver nanoparticles and their applications: about future directions. A Review. Bionanoscience 8:5–16. https://doi.org/10.1007/s12668-017-0413-3

Abele-Horn M, Schupfner B, Emmerling P, Waldner H, Göring H (2000) Persistent wound infection after herniotomy associated with small-colony variants of *Staphylococcus aureus*. Infection 28:53–54. https://doi.org/10.1007/s150100050014

Ahmad T, Wani IA, Manzoor N, Asiri AM (2013) Biosynthesis structural characterization and antimicrobial activity of gold and silver. Coll Surf B 107:227–234

Alfuraydi AA, Devanesan S, Al-ansari M, Alsalhi MS, Ranjitsingh AJ (2019) Eco-friendly green synthesis of silver nanoparticles from the sesame oil cake and its potential anticancer and antimicrobial activities. J Photochem Photobiol B Biol 192:83–89. https://doi.org/10.1016/j.jphotobiol.2019.01.011

Asati S, Chaudhary U (2017) Prevalence of biofilm producing aerobic bacterial isolates in burn wound infections at a tertiary care hospital in northern India. Ann Burns Fire Disasters 30:39–42

Bergonzi C, d'Ayala GG, Elviri L, Laurienzo P, Bandiera A, Catanzano O (2020) Alginate/human elastin-like polypeptide composite films with antioxidant properties for potential wound healing application. Int J Biol Macromol 164:586–596. https://doi.org/10.1016/j.ijbiomac.2020.07.084

Chambers ES, Vukmanovic-Stejic M (2020) Skin barrier immunity and ageing. Immunology. https://doi.org/10.1111/imm.13152

Ciecholewska-Juśko D, Żywicka A, Junka A, Drozd R, Sobolewski P, Migdał P, Kowalska U, Toporkiewicz M, Fijałkowski K (2021) Superabsorbent crosslinked bacterial cellulose biomaterials for chronic wound dressings. Carbohydr Polym. https://doi.org/10.1016/j.carbpol.2020.117247

Da Silva FAG, Queiroz JC, Macedo ER, Fernandes AWC, Freire NB, Da Costa MM, De Oliveira HP (2016) Antibacterial behavior of polypyrrole: the influence of morphology and additives incorporation. Mater Sci Eng C 62:317–322. https://doi.org/10.1016/j.msec.2016.01.067

da Silva FAG, Alcaraz-Espinoza JJ, da Costa MM, de Oliveira HP (2019) Low intensity electric field inactivation of Gram-positive and Gram-negative bacteria via metal-free polymeric composite. Mater Sci Eng C. https://doi.org/10.1016/j.msec.2019.02.027

dos Santos MR, Alcaraz-Espinoza JJ, da Costa MM, de Oliveira HP (2018) Usnic acid-loaded polyaniline/polyurethane foam wound dressing: preparation and bactericidal activity. Mater Sci Eng C. https://doi.org/10.1016/j.msec.2018.03.019

Dzimitrowicz A, Berent S, Motyka A, Jamroz P, Kurcbach K, Sledz W, Pohl P (2016) Comparison of the characteristics of gold nanoparticles synthesized using aqueous plant extracts and natural plant essential oils of Eucalyptus globulus and Rosmarinus officinalis. Arab J Chem 12:4795–4805. https://doi.org/10.1016/j.arabjc.2016.09.007

Estevez MB, Raffaelli S, Mitchell SG, Faccio R, Alborés S (2020) Biofilm eradication using biogenic silver nanoparticles. Molecules 25:2023. https://doi.org/10.3390/molecules25092023

Evelhoch SR (2020) Biofilm and chronic nonhealing wound infections. Surg Clin North Am. https://doi.org/10.1016/j.suc.2020.05.004

Fazli M, Bjarnsholt T, Kirketerp-Møller K, Jørgensen B, Andersen AS, Krogfelt KA, Givskov M, Tolker-Nielsen T (2009) Nonrandom

distribution of pseudomonas aeruginosa and *Staphylococcus aureus* in chronic wounds. J Clin Microbiol 47:4084–4089. https://doi.org/10.1128/JCM.01395-09

Ferrag C, Li S, Jeon K, Andoy NM, Sullan RMA, Mikhaylichenko S, Kerman K (2021) Polyacrylamide hydrogels doped with different shapes of silver nanoparticles: antibacterial and mechanical properties. Coll Surf B Biointerfaces 197:111397. https://doi.org/10.1016/j.colsurfb.2020.111397

Gavade NL, Kadam AN, Suwarnkar MB, Ghodake VP, Garadkar KM (2015) Spectrochimica acta part a: molecular and biomolecular spectroscopy biogenic synthesis of multi-applicative silver nanoparticles by using Ziziphus Jujuba leaf extract 136: 953–960https://doi.org/10.1016/j.saa.2014.09.118

Granbohm H, Larismaa J, Ali S, Johansson LS, Hannula SP (2018) Control of the size of silver nanoparticles and release of silver in heat treated SiO_2-Ag composite powders. Materials (basel). https://doi.org/10.3390/ma11010080

Guimarães ML, da Silva FAG, da Costa MM, de Oliveira HP (2020) Green synthesis of silver nanoparticles using Ziziphus joazeiro leaf extract for production of antibacterial agents. Appl Nanosci. https://doi.org/10.1007/s13204-019-01181-4

Howaili F, Mashreghi M, Shahri NM, Kompany A, Jalal R (2020) Development and evaluation of a novel beneficent antimicrobial bioscaffold based on animal waste-fish swim bladder (FSB) doped with silver nanoparticles. Environ Res 188:109823. https://doi.org/10.1016/j.envres.2020.109823

Hu Z, Yang P, Zhou C, Li S, Hong P (2017) Marine collagen peptides from the skin of nile tilapia (*Oreochromis niloticus*): characterization and wound healing evaluation. 15:102. https://doi.org/10.3390/md15040102

Hussain Z, Thu HE, Katas H, Bukhari SNA (2017) Hyaluronic acid-based biomaterials: a versatile and smart approach to tissue regeneration and treating traumatic, surgical, and chronic wounds. Polym Rev 57:594–630. https://doi.org/10.1080/15583724.2017.1315433

James GA, Swogger E, Wolcott R, Pulcini ED, Secor P, Sestrich J, Costerton JW, Stewart PS, James G (2008) Biofilms in chronic wounds. Wiley Online Libr 16:37–44. https://doi.org/10.1111/j.1524-475X.2007.00321.x

Jorge de Souza TA, Rosa Souza LR, Franchi LP (2019) Silver nanoparticles: an integrated view of green synthesis methods, transformation in the environment, and toxicity. Ecotoxicol Environ Saf 171:691–700. https://doi.org/10.1016/J.ECOENV.2018.12.095

Le Ouay B, Stellacci F (2015) Science direct antibacterial activity of silver nanoparticles: a surface science insight. Nano Today 10:339–354. https://doi.org/10.1016/j.nantod.2015.04.002

Li R, Chen Z, Ren N, Yixuan W, Wang Y, Yu F (2019) Biosynthesis of silver oxide nanoparticles and their photocatalytic and antimicrobial activity evaluation for wound healing applications in nursing care. J Photochem Photobiol B Biol. https://doi.org/10.1016/j.jphotobiol.2019.111593

Lima EM, de Moraes Filho MO, Costa BA, Nunes Alves APN, de Moraes MEA, do Nascimento Uchôa AM, Martins CB, de Jesus Pinheiro Gomes Bandeira T, Rocha Rodrigues FA, Koscky Paier CR, Lima FC, Silva FR (2020) Lyophilised tilapia skin as a xenograft for superficial partial thickness burns: a novel preparation and storage technique. J Wound Care 29:598–602.https://doi.org/10.12968/jowc.2020.29.10.598

Maciel MVDO, Almeida ADR, Machado MH, Melo APZ, da Rosa CG, Freitas DZ, Noronha CM, Teixeira GL, Armas RD, Barreto PLM (2019) *Syzygium aromaticum* L. (Clove) essential oil as a reducing agent for the green synthesis of silver nanoparticles. Open J Appl Sci. https://doi.org/10.4236/ojapps.2019.92005

Maghimaa M, Ali S (2020) Biology Green synthesis of silver nanoparticles from *Curcuma longa* L. and coating on the cotton fabrics for antimicrobial applications and wound healing activity. J Photochem Photobiol B Biol 204:111806. https://doi.org/10.1016/j.jphotobiol.2020.111806

Mao Y, Li P, Yin J, Bai Y, Zhou H, Lin X, Yang H, Yang L (2021) Starch-based adhesive hydrogel with gel-point viscoelastic behavior and its application in wound sealing and hemostasis. J Mater Sci Technol 63:228–235. https://doi.org/10.1016/j.jmst.2020.02.071

Miranda M, Brandt C (2001) Nile tilapia skin xenograft versus silver-based hydrofiber dressing in the treatment of second-degree burns in adults. Revista Brasileira De Cirurgia Plástica 34:79–85. https://doi.org/10.5935/2177-1235.2019rbcp0012

Mottola C, Matias CS, Mendes JJ, Melo-Cristino J, Tavares L, Cavaco-Silva P, Oliveira M (2016) Susceptibility patterns of *Staphylococcus aureus* biofilms in diabetic foot infections. BMC Microbiol. https://doi.org/10.1186/s12866-016-0737-0

Mukundan D, Mohankumar R, Vasanthakumari R (2005) Green synthesis of gold nanoparticles using leaves extract of bauhinia tomentosa linn and invitro anticancer activity. IJIRSE 2:375–380

Negut I, Grumezescu V, Grumezescu AM (2018) Treatment strategies for infected wounds. Molecules. https://doi.org/10.3390/molecules23092392

Nishanthi R, Malathi S, Paul SJ, Palani P (2018) Green synthesis and characterization of bioinspired silver, gold and platinum nanoparticles and evaluation of their synergistic antibacterial activity after combining with different classes of antibiotics. Mater Sci Eng C. https://doi.org/10.1016/j.msec.2018.11.050

Ochoa M, Rahimi R, Zhou J, Jiang H, Yoon CK, Maddipatla D, Narakathu BB, Jain V, Oscai MM, Morken TJ, Oliveira RH, Campana GL, Cummings OW, Zieger MA, Sood R, Atashbar MZ, Ziaie B (2020) Integrated sensing and delivery of oxygen for next-generation smart wound dressings. Microsyst Nanoeng. https://doi.org/10.1038/s41378-020-0141-7

Ouyang QQ, Hu Z, Lin ZP, Quan WY, Deng YF, Li SD, Li PW, Chen Y (2018) Chitosan hydrogel in combination with marine peptides from tilapia for burns healing. Int J Biol Macromol 112:1191–1198. https://doi.org/10.1016/j.ijbiomac.2018.01.217

Roy S, Bisaria K, Nagabooshanam S, Selvam A, Chakrabarti S, Wadhwa S, Singh R, Mathur A, Davis J (2021) An electroanalytical paper-based wound dressing using ZIF-67/C3N4 nanocomposite towards the monitoring of staphylococcus aureus in diabetic foot ulcer. IEEE Sens J 21:1215–1221. https://doi.org/10.1109/JSEN.2020.3018019

Salaheldin HI, Almalki MHK, Osman GEH (2017) Green synthesis of silver nanoparticles using bovine skin gelatin and its antibacterial effect on clinical bacterial isolates. IET Nanobiotechnol 11:420–425. https://doi.org/10.1049/iet-nbt.2016.0126

Schierle CF, De La Garza M, Mustoe TA, Galiano RD (2009) Staphylococcal biofilms impair wound healing by delaying reepithelialization in a murine cutaneous wound model. Wound Repair Regen 17:354–359. https://doi.org/10.1111/j.1524-475X.2009.00489.x

Sharifi S, Hajipour MJ, Gould L, Mahmoudi M (2021) Nanomedicine in healing chronic wounds: opportunities and challenges. Mol Pharm. https://doi.org/10.1021/acs.molpharmaceut.0c00346

Song W-K, Liu D, Sun L-L, Li B-F, Hou H (2019) Marine drugs physicochemical and biocompatibility properties of type I collagen from the skin of Nile Tilapia (*Oreochromis niloticus*) for Biomedical Applications. Mar. Drugs 17:137. https://doi.org/10.3390/md17030137

Song Z, Liu H, Liwen C, Leilei C, Zhou C, Hong P, Deng C (2021) Characterization and comparison of collagen extracted from the skin of the Nile tilapia by fermentation and chemical pretreatment. Food Chem 340:128139. https://doi.org/10.1016/j.foodchem.2020.128139

Sun L, Li B, Song W, Zhang K, Fan Y, Hou H (2020) Comprehensive assessment of Nile tilapia skin collagen sponges as hemostatic

dressings. Mater Sci Eng C 109:110532. https://doi.org/10.1016/j.msec.2019.110532

Sutthanont N, Attrapadung S, Nuchprayoon S (2019) Larvicidal activity of synthesized silver nanoparticles from curcuma zedoaria essential oil against culex quinquefasciatus. Insects. https://doi.org/10.3390/insects10010027

Tang S, Zheng J (2018) Antibacterial activity of silver nanoparticles: structural effects. Adv Healthc Mater. https://doi.org/10.1002/adhm.201701503

Tulinski M, Jurczyk M (2017) Nanomaterials synthesis methods. Metrol Stand Nanotechnol 75–98. https://doi.org/10.1002/9783527800308.ch4

van Wamel WJB (2017) Staphylococcus aureus infections, some second thoughts. Curr Opin Infect Dis 30:303–308. https://doi.org/10.1097/QCO.0000000000000366

Veisi H, Dadres N, Mohammadi P, Hemmati S (2019) Materials Science and Engineering C Green synthesis of silver nanoparticles based on oil-water interface method with essential oil of orange peel and its application as nanocatalyst for A 3 coupling. Mater Sci Eng C 105:110031. https://doi.org/10.1016/j.msec.2019.110031

Vilas V, Philip D, Mathew J (2014) Catalytically and biologically active silver nanoparticles synthesized using essential oil. Spectrochim Acta Part a Mol Biomol Spectrosc 132:743–750. https://doi.org/10.1016/j.saa.2014.05.046

Vilas V, Philip D, Mathew J (2016) Biosynthesis of Au and Au/Ag alloy nanoparticles using Coleus aromaticus essential oil and evaluation of their catalytic, antibacterial and antiradical activities. J Mol Liq. https://doi.org/10.1016/j.molliq.2016.05.066

Wang T, Yang L, Wang G, Han L, Chen K, Liu P, Xu S, Li D, Xie Z, Mo X, Wang L, Liang H, Liu X, Zhang S, Gao Y (2021) Biocompatibility, hemostatic properties, and wound healing evaluation of tilapia skin collagen sponges. J Bioact Compat Polym 36:44–58. https://doi.org/10.1177/0883911520981705